

Joint In-Band Backhauling and Interference Mitigation in 5G Heterogeneous Networks

Trung Kien Vu, *Student Member, IEEE*, Mehdi Bennis, *Senior Member, IEEE*,
Sumudu Samarakoon, *Student Member, IEEE*, M  rouane Debbah, *Fellow, IEEE*, and Matti Latva-aho, *Senior Member, IEEE*,

Abstract—In this paper, we study the problem of joint in-band backhauling and interference mitigation in 5G heterogeneous networks (HetNets) in which a massive multiple-input multiple-output (MIMO) macro cell base station equipped with a large number of antennas, overlaid with self-backhauled small cells is assumed. This problem is cast as a network utility maximization subject to wireless backhaul constraints. Due to the non-tractability of the problem, we first resort to random matrix theory to get a closed-form expression of the achievable rate and transmit power in the asymptotic regime, i.e., as the number of antennas and users grows large. Subsequently, leveraging the framework of stochastic optimization, the problem is decoupled into dynamic scheduling of macro cell users and backhaul provisioning of small cells as a function of interference and backhaul links. Via simulations, we evaluate the performance gains of our proposed framework under different network architectures and low/high frequency bands. Our proposed HetNet method achieves the achievable average UE throughput of 1.7 Gbps as well as ensures 1 Gbps cell-edge UE throughput when serving 200 UEs per km² at 28 GHz with 1 GHz bandwidth. In ultra-dense network, the UE throughput at 28 GHz achieves 62× gain as compared to 2.4 GHz. Moreover, we show that there exists an $\mathcal{O}(1/\nu), \mathcal{O}(\nu)$ utility-queue backlog tradeoff with any arbitrary non-negative ν .

I. INTRODUCTION

The demand for massive data traffic has grown due to the exponential increase in the number of mobile broadband subscribers such as smartphones and tablets. To handle these relentless demands, in the next generation wireless networks, a number of candidate solutions include: 1) higher frequency spectrum (centimeter and millimeter-wave (mmWave)); 2) advanced spectral-efficiency techniques (massive MIMO); and 3) ultra-dense small cell deployments [1]. Massive MIMO plays an important role in wireless networks due to an improvement in energy and spectral efficiency [2]. The basic concept of massive MIMO assumes a macro base station (MBS) equipped with a few hundreds antennas simultaneously serving tens of macro user equipments (MUEs). On the other hand, ultra dense SC deployment provides an effective solution to increase network capacity. In parallel to that, recent advances in full-duplex (FD) enables doubling spectral efficiency and lowering latency, which is another promising technique [3].

Manuscript received March 15, 2016; revised and accepted April 19, 2016. Date of publication May 20, 2016; This work was supported in part by the Finnish Funding Agency for Technology and Innovation (Tekes), Nokia, Huawei, Anite, in part by the Academy of Finland funding through the grant 284704, and in part by the ERC Starting Grant 305123 MORE (Advanced Mathematical Tools for Complex Network Engineering).

T. K. Vu, M. Bennis, S. Samarakoon, and M. Latva-aho are with the Centre for Wireless Communications, University of Oulu, Oulu 90014, Finland (e-mail: trungkien.vu@oulu.fi; mehdi.bennis@oulu.fi; sumudu.samarakoon@oulu.fi; matti.latva-aho@oulu.fi).

M. Debbah is with the Large Networks and System Group (LANEAS), CentraleSup  lec, Universit   Paris-Saclay, Gif-sur-Yvette, France and is with the Mathematical and Algorithmic Sciences Laboratory, Huawei France R&D, Paris, France (e-mail: merouane.debbah@huawei.com).

Citation information: In proceeding of 2016 IEEE European Wireless

The combination of massive MIMO and ultra-dense SCs holds the promise of ensuring high capacity improvement and constitutes the main motivation of this work. Recently, SC wireless backhaul in massive MIMO was studied in [3], [4] showing the efficiency of combining massive MIMO and wireless backhaul-based small cell networks focusing on minimizing power consumption. However, the key challenge of how to dynamically optimize the overall network performance taking into account the backhaul dynamics, and scheduling has not been addressed. The main contribution of this work is to study the problem of joint scheduling, interference mitigation, and in-band wireless backhauling. We design precoders to alleviate both co-tier and cross tier interference and dynamically provide wireless backhauling to SCs. An operation mode is proposed to dynamically control the interference among adjacent SCs. By invoking results from random matrix theory (RMT), we derive a closed-form expression of the signal-to-interference-plus-noise-ratio (SINR) when the numbers of MBS antennas and users grow very large. A network utility optimization problem is formulated to maximize the total network throughput subject to dynamically varying wireless backhaul. Leveraging the framework of stochastic optimization, the problem is decoupled into several subproblems. The mixed-integer non-convex subproblem is solved by applying the framework of successive convex approximation (SCA). A performance evaluation is carried out for different network deployments at low/high frequency bands.

The rest of this paper is organized as follows. Section II describes the system model and Section III formulates the problem of scheduling and interference mitigation. Section IV adopts the Lyapunov optimization framework and the SCA method used to solve the problem. In Section V, the simulation results are presented and Section VI concludes the paper.

II. SYSTEM MODEL

A. System Model

We consider the downlink (DL) transmission of a HetNet scenario as shown in Fig. 1 in which a MBS b_0 is underlaid with a set of uniformly deployed S SCs, $\mathcal{S} = \{b_s | s \in \{1, \dots, S\}\}$. Let $\mathcal{B} = \{b_0\} \cup \mathcal{S}$ denote the set of all base stations (BSs), where $|\mathcal{B}| = 1 + S$. The MBS is equipped with N number of antennas and serves a set of single-antenna M MUEs $\mathcal{M} = \{1, \dots, M\}$. Let $\mathcal{K} = \mathcal{M} \cup \mathcal{S}$ denote the set of b_0 's associated users, where $|\mathcal{K}| = K = M + S$. SCs are assumed to be FD capable with perfect self-interference cancellation (SIC) capabilities¹. Each SC is equipped with two antennas: the receiving antenna is used for the wireless backhaul and the transmitting antenna to serve its single-antenna small cell user equipment (SUE)². Let $\mathcal{C} = \{c_1, c_2, \dots, c_S\}$ denote the set of SUEs, where $|\mathcal{C}| = S$. We assume closed-access

¹The case of imperfect SIC is left for future work.

²In general, one SC base station can serve more than one SUE. Without loss of generality, one SUE with higher traffic demand can be considered as multiple SUEs with lower traffic demand. More SUEs per SC is left for future work.

policy where SCs serve their own users. Co-channel time-division duplexing (TDD) protocol is considered in which the MBS and SCs share the entire bandwidth, and do the DL transmission at the same time. In this work, we consider a large number of antennas at the MBS and a dense deployment of MUEs and SCs, such that $M, N, S \gg 1$.

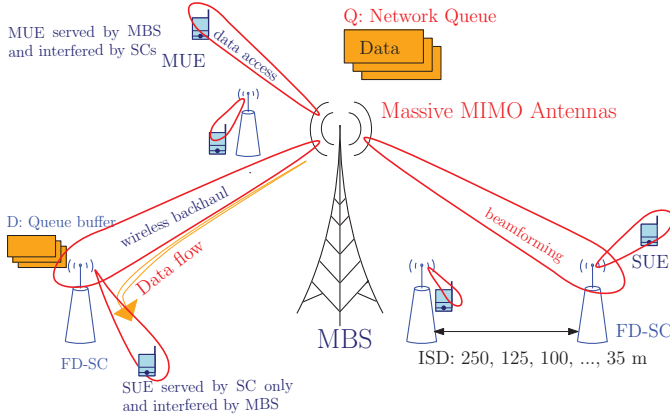


Fig. 1: Integrated Access and Backhaul Architecture for 5G network.

B. Channel Model

We denote $\mathbf{h}_m^{(b_0)} = [h_m^{(b_0,1)}, h_m^{(b_0,2)}, \dots, h_m^{(b_0,N)}]^T \in \mathbb{C}^{N \times 1}$ the propagation channels between the m th MUE and the antennas of the MBS b_0 in which $h_m^{(b_0,n)}$ is the channel between the m th MUE and n th MBS antenna. Let $\mathbf{H}^{(b_0),M} = [\mathbf{h}_1^{(b_0)}, \mathbf{h}_2^{(b_0)}, \dots, \mathbf{h}_M^{(b_0)}] \in \mathbb{C}^{N \times M}$ denote the channel matrix between all MUEs and the MBS antennas. Moreover, we assume imperfect channel state information (CSI) for MUEs due to mobility and we denote $\hat{\mathbf{H}}^{(b_0),M} = [\hat{\mathbf{h}}_1^{(b_0)}, \hat{\mathbf{h}}_2^{(b_0)}, \dots, \hat{\mathbf{h}}_M^{(b_0)}] \in \mathbb{C}^{N \times M}$ as the estimate of $\mathbf{H}^{(b_0),M}$ in which the imperfect CSI can be modeled as [5]:

$$\hat{\mathbf{h}}_m^{(b_0)} = \sqrt{N\Theta_m^{(b_0)}} \hat{\mathbf{w}}_m^{(b_0)}, \quad (1)$$

where $\hat{\mathbf{w}}_m^{(b_0)} = \sqrt{1 - \tau_m^2} \mathbf{w}_m^{(b_0)} + \tau_m \mathbf{z}_m^{(b_0)}$ is the estimate of the small-scale fading channel matrix and $\Theta_m^{(b_0)}$ is the spatial channel correlation matrix that accounts for path loss and shadow fading. Here, $\mathbf{w}_m^{(b_0)}$ and $\mathbf{z}_m^{(b_0)}$ are the real channel and the channel noise, respectively, modeled as Gaussian random matrix with zero mean and variance $1/N$. The channel estimate error of MUE m is denoted by τ_m ; in case of perfect CSI, $\tau_m = 0$. Similarly, let $\mathbf{H}^{(b_0),S} \in \mathbb{C}^{N \times S}$ and $\mathbf{H}^{(b_0),C} \in \mathbb{C}^{N \times S}$ denote the channel matrices from the MBS antennas to SCs and SUEs, respectively. Let $h_i^{(b_s)}$ denote the channel propagation from SC b_s to any receiver i . Let c_s denote the SUE served by the SC b_s .

III. JOINT ACCESS/BACKHAUL SCHEDULING AND INTERFERENCE MITIGATION PROBLEM FORMULATION

We address the problem of DL scheduling at the MBS to simultaneously provide data transmission to MUEs and wireless backhaul to SCs. We define the scheduling vector $\mathbf{l}(t) = (l_1(t), l_2(t), \dots, l_K(t))$ to determine the subset of users served at time slot t , where $l_k(t) = 1$ means user k is served at time slot t and $l_k(t) = 0$ otherwise.

A. Downlink Transmission Signal

The MBS serves two types of users: MUEs and SCs, let $p_m^{(b_0)}$, $p_s^{(b_0)}$, and $P^{(b_0)}$ denote the DL MBS transmit power assigned to MUE m , SC b_s , and the maximum transmit

power at the MBS, respectively. Let $p_{c_s}^{(b_s)}$ denote the DL transmit power of SC b_s assigned to SUE c_s . Although SC exploits FD capability to double capacity, SC causes unwanted FD interference including cross-tier interference to adjacent MUEs (or other SCs) and co-tier interference to other SUEs. Moreover, inspired by [6], we invoke RMT to get closed-form expression for the user data rate as $N, K \gg 1$. In order to convert the interference channel to multiple-input single-output (MISO) channel, we design a precoder at MBS and propose an operation mode policy to control FD interference due to the SC DL transmissions such that the total FD interference at receiver is treated as noise.

Definition 1. [Operation Mode Policy] We define β as the operation mode to control the SC transmission to reduce FD interference. The operation mode is expressed as $\beta(t) = \{\beta^{(b_s)}(t) \mid \beta^{(b_s)}(t) \in \{0, 1\}, \forall s \in \mathcal{S}\}$. If SC b_s operates in FD mode, then $\beta^{(b_s)}(t) = 1$. When SC b_s operates in half-duplex (HD) mode, i.e., $\beta^{(b_s)}(t) = 0$.

We assume that the MBS uses a precoding scheme, $\mathbf{V} = [\mathbf{v}_1, \mathbf{v}_2, \dots, \mathbf{v}_K] \in \mathbb{C}^{N \times K}$. We apply the technique in [7] to design the precoder $\mathbf{V} = \mathbf{U}\mathbf{T}$, where $\mathbf{U} \in \mathbb{C}^{N \times N_i}$ and $\mathbf{T} \in \mathbb{C}^{N_i \times K}$ are used to control cross-tier and co-tier interference, respectively. Here, N_i antennas are used to mitigate the cross-tier interference with $N_i < N$, where the subscript i stands for ‘‘interference’’. The precoder \mathbf{U} is chosen such that

$$\mathbf{U}^\dagger \sum_{s=1}^S \beta^{(b_s)} \Theta_{c_s}^{(b_0)} = \mathbf{0}, \quad (2)$$

where $\Theta_{c_s}^{(b_0)} \in \mathbb{C}^{N \times N}$ is the correlation matrix between MBS antennas and SUE c_s . Note that $\beta^{(b_s)}$ determines that SUE c_s is served or not, and \mathbf{U}^\dagger denotes the Hermitian transpose of matrix \mathbf{U} . The precoder \mathbf{T} is designed to adapt to the real time CSI based on $\hat{\mathbf{H}}^\dagger \mathbf{U} \in \mathbb{C}^{K \times N_i}$, where $\hat{\mathbf{H}} = [\hat{\mathbf{h}}_k^{(b_0)}]_{k \in \mathcal{K}}$. In this paper, we consider the regularized zero-forcing (RZF) precoding³ given by $\mathbf{T} = (\mathbf{U}^\dagger \hat{\mathbf{H}}^\dagger \hat{\mathbf{H}} \mathbf{U} + N\alpha \mathbf{I}_{N_i})^{-1} \mathbf{U}^\dagger \hat{\mathbf{H}}^\dagger$, where the regularization parameter $\alpha > 0$ is scaled by N to ensure that the matrix $\mathbf{U}^\dagger \hat{\mathbf{H}}^\dagger \hat{\mathbf{H}} \mathbf{U} + N\alpha \mathbf{I}_{N_i}$ is well conditioned as $N \rightarrow \infty$. The precoder \mathbf{T} is chosen to satisfy the power constraint $\text{Tr}(\mathbf{P}\mathbf{T}^\dagger \mathbf{T}) \leq P^{(b_0)}$, where $\mathbf{P} = \text{diag}(p_1^{(b_0)}, p_2^{(b_0)}, \dots, p_K^{(b_0)})$. By utilizing a massive number of antennas at MBS, a large spatial degree of freedom is partly utilized to serve MUEs and FD-enabled SCs, while the remaining degrees of freedom are used to mitigate cross-tier interference. In massive MIMO system, the total number of antennas is considered as the degree of freedom [2]. Hence, we have the antenna constraint for scheduling and operation mode such that $\sum_{k=1}^K l_k(t) + \sum_{s=1}^S \beta^{(b_s)}(t) \leq N$. For notational simplicity, we remove the time dependency from the symbols throughout the discussion. The received signal $y_m^{(b_0)}$ at each MUE $m \in \mathcal{M}$ at time instant t is given by

$$y_m^{(b_0)} = l_m \sqrt{p_m^{(b_0)}} \mathbf{h}_m^{(b_0)\dagger} \mathbf{v}_m x_m^{(b_0)} + \underbrace{\sum_{s=1}^S \beta^{(b_s)} \sqrt{p_{c_s}^{(b_s)}} h_m^{(b_s)\dagger} x_{c_s}^{(b_s)}}_{\text{cross-tier interference}} + \underbrace{\sum_{k=1, k \neq m}^K l_k \sqrt{p_k^{(b_0)}} \mathbf{h}_m^{(b_0)\dagger} \mathbf{v}_k x_k^{(b_0)}}_{\text{co-tier interference}} + \eta_m, \quad (3)$$

where $x_m^{(b_0)}$ is the signal symbol from the MBS to the MUE m , $\eta_m \sim \mathcal{CN}(0, 1)$ is the thermal noise at MUE m , and \mathbf{v}_m is the precoding vectors of MUE m . $x_{c_s}^{(b_s)}$ is the transmit signal symbol from SC b_s to SUE c_s .

³Other precoders are left for future work.

At time instant t , the received signal $y_s^{(b_0)}$ at each SC $b_s \in \mathcal{S}$ suffers from self-interference, cross-tier interference, and co-tier interference which is given by

$$y_s^{(b_0)} = l_s \sqrt{p_s^{(b_0)}} \mathbf{h}_s^{(b_0)\dagger} \mathbf{v}_s x_s^{(b_0)} + \underbrace{\beta^{(b_s)} \sqrt{p_{c_s}^{(b_s)}} h_s^{(b_s)\dagger} x_{c_s}^{(b_s)}}_{\text{self-interference}} + \underbrace{\sum_{s'=1, s' \neq s}^S \beta^{(b_{s'})} \sqrt{p_{c_{s'}}^{(b_{s'})}} h_s^{(b_{s'})\dagger} x_{c_{s'}}^{(b_{s'})}}_{\text{cross-tier interference}} + \underbrace{\sum_{k=1, k \neq s}^K l_k \sqrt{p_k^{(b_0)}} \mathbf{h}_s^{(b_0)\dagger} \mathbf{v}_k x_k^{(b_0)}}_{\text{co-tier interference}} + \eta_s, \quad (4)$$

where $\eta_s \sim \mathcal{CN}(0, 1)$ is the thermal noise of the SC b_s . In this work, the FD capability is leveraged at SCs.

The received signal at SUE c_s from its serving SC b_s is interfered by the DL signals from other SCs and the MBS. At time instant t , it is given by

$$y_{c_s}^{(b_s)} = \beta^{(b_s)} \sqrt{p_{c_s}^{(b_s)}} h_{c_s}^{(b_s)\dagger} x_{c_s}^{(b_s)} + \underbrace{\sum_{k=1}^K l_k \sqrt{p_k^{(b_0)}} \mathbf{h}_{c_s}^{(b_0)\dagger} \mathbf{v}_k x_k^{(b_0)}}_{\text{cross-tier interference}} + \underbrace{\sum_{s'=1, s' \neq s}^S \beta^{(b_{s'})} \sqrt{p_{c_{s'}}^{(b_{s'})}} h_{c_s}^{(b_{s'})\dagger} x_{c_{s'}}^{(b_{s'})}}_{\text{co-tier interference}} + \eta_{c_s}, \quad (5)$$

where $x_{c_s}^{(b_s)}$ is the transmit data symbol from the SC b_s to its own SUE c_s and $\eta_{c_s} \sim \mathcal{CN}(0, 1)$ is the SUE thermal noise.

According to (2)-(5), the SINRs of MUE $m \in \mathcal{M}$, SC $b_s \in \mathcal{S}$, and SUE c_s are given by:

$$\gamma_m^{(b_0)} = \frac{l_m p_m^{(b_0)} |\mathbf{h}_m^{(b_0)\dagger} \mathbf{v}_m|^2}{\sum_{k \neq m} l_k p_k^{(b_0)} |\mathbf{h}_m^{(b_0)\dagger} \mathbf{v}_k|^2 + \sum_s \beta^{(b_s)} p_{c_s}^{(b_s)} |h_m^{(b_s)\dagger}|^2 + 1} \quad (6)$$

$$\gamma_s^{(b_0)} = \frac{l_s p_s^{(b_0)} |\mathbf{h}_s^{(b_0)\dagger} \mathbf{v}_s|^2}{\sum_{k \neq s} l_k p_k^{(b_0)} |\mathbf{h}_s^{(b_0)\dagger} \mathbf{v}_k|^2 + \sum_{s' \neq s} \beta^{(b_{s'})} p_{c_{s'}}^{(b_{s'})} |h_s^{(b_{s'})\dagger}|^2 + 1}, \quad (7)$$

$$\gamma_{c_s}^{(b_s)} = \frac{\beta^{(b_s)} p_{c_s}^{(b_s)} |h_{c_s}^{(b_s)\dagger}|^2}{\sum_{s' \neq s} \beta^{(b_{s'})} p_{c_{s'}}^{(b_{s'})} |h_{c_s}^{(b_{s'})\dagger}|^2 + 1}. \quad (8)$$

B. Downlink Scheduling Problem

We consider a joint optimization of scheduling \mathbf{l} , operation mode β , interference mitigation \mathbf{U} , and transmit power allocation $\mathbf{p} = (p_1^{(b_0)}, p_2^{(b_0)}, \dots, p_K^{(b_0)})$ that satisfies the transmit power budget of MBS, i.e., $\text{Tr}(\mathbf{P}\mathbf{T}^\dagger\mathbf{T}) \leq P^{(b_0)}$. We define $\zeta_i^{(b_s)} = \frac{p_{c_s}^{(b_s)} |h_i^{(b_s)\dagger}|^2}{|\eta_i|^2}$ and ϵ_o as the FD interference to noise ratio (INR) from SC b_s to any scheduled receiver i , and the allowed FD INR threshold, respectively. The FD INR threshold is defined such that $\sum_{i=1}^K \sum_{s=1}^S \zeta_i^{(b_s)} \leq \epsilon_o$ in which the total FD interference is considered as noise. Under the operation mode policy, we schedule the receiver i and enable the transmission of SC b_s as long as $\sum_{i=1}^K \sum_{s=1}^S l_i \beta^{(b_s)} \zeta_i^{(b_s)} \leq \epsilon_o$.

Let $\Lambda^o = \{\mathbf{l}, \beta\}$ be a composite control variable of scheduling and operation mode. We define $\Lambda = \{\Lambda^o, \mathbf{U}, \mathbf{p}\}$ as a composite control variable, which adapts to the spatial channel correlation matrix Θ . For a given Λ that satisfies (2)

and operation mode policy, the respective Ergodic data rates of MUE, SC, and SUE are:

$$r_m(\Lambda|\Theta) = \mathbb{E}[\log(1 + \gamma_m^{(b_0)})], \\ r_s(\Lambda|\Theta) = \mathbb{E}[\log(1 + \gamma_s^{(b_0)})], \text{ and} \\ r_{c_s}(\Lambda|\Theta) = \mathbb{E}[\log(1 + \gamma_{c_s}^{(b_s)})].$$

Definition 2. For any vector $\mathbf{x}(t) = (x_1(t), \dots, x_K(t))$, let $\bar{\mathbf{x}} = (\bar{x}_1, \dots, \bar{x}_K)$ denote the time average expectation of $\mathbf{x}(t)$, where $\bar{\mathbf{x}} \triangleq \lim_{t \rightarrow \infty} \frac{1}{t} \sum_{\tau=0}^{t-1} \mathbb{E}[\mathbf{x}(\tau)]$. Similarly, $\bar{\mathbf{r}} \triangleq \lim_{t \rightarrow \infty} \frac{1}{t} \sum_{\tau=0}^{t-1} \mathbb{E}[\mathbf{r}(\tau)]$ denotes the time average expectation of the Ergodic data rate.

For a given composite control variable Λ that adapts to the spatial channel correlation matrix Θ , the average data rate region is defined as the convex hull of the average data rate of users, which is expressed as:

$$\mathcal{R} \triangleq \{\bar{\mathbf{r}}(\Lambda|\Theta) \in \mathbf{R}_+^K \mid \mathbf{l} \in \{0, 1\}^K, \beta \in \{0, 1\}^S, \\ \sum_{k=1}^K l_k + \sum_{s=1}^S \beta^{(b_s)} \leq N, \\ \sum_{i=1}^K \sum_{s=1}^S l_i \beta^{(b_s)} \zeta_i^{(b_s)} \leq \epsilon_o, \\ \text{Tr}(\mathbf{P}\mathbf{T}^\dagger\mathbf{T}) \leq P^{(b_0)}, \\ \mathbf{U}^\dagger \sum_{s=1}^S \beta^{(b_s)} \Theta_{c_s}^{(b_0)} = 0\},$$

where $\bar{\mathbf{r}}(\Lambda|\Theta) = (\bar{r}_1(\Lambda|\Theta), \dots, \bar{r}_K(\Lambda|\Theta))^T$. Following the results from [8], the boundary points of the rate regime with total power constraint and no self-interference are Pareto-optimal⁴. Moreover, according to [9, Proposition 1], if the INR covariance matrices approach the identity matrix, the Pareto rate regime of the MIMO interference system is convex. Hence, the rate regime is Pareto-optimal, and thus, convex under above constraints.

Let us assume that SCs act as relays to forward data to the SUEs. If the MBS transmits data to SC b_s , but the transmission of SC b_s is disabled, it cannot serve its SUE. Hence, we define $\mathbf{D}(t) = (D_1(t), D_2(t), \dots, D_S(t))$ as a data queue at SCs, where at each time slot t , the wireless backhaul queue at SC b_s is

$$D_s(t+1) = \max[D_s(t) + r_s(t) - r_{c_s}(t), 0]. \quad (9)$$

We define the network utility function f_0 to be non-decreasing, concave over the convex region \mathcal{R} for a given Θ . The objective is to maximize the network utility under wireless backhaul queue constraints and imperfect CSI. Thus, the network utility maximization (NUM) problem is given by,

$$\max_{\bar{\mathbf{r}}} f_0(\bar{\mathbf{r}}) \quad (10a)$$

$$\text{subject to } \bar{\mathbf{r}} \in \mathcal{R}, \quad (10b)$$

$$\bar{\mathbf{D}} < \infty. \quad (10c)$$

where $f_0(\bar{\mathbf{r}}) = \sum_{k=1}^K \omega_k(t) f(\bar{r}_k)$, and $\omega_k(t) \geq 0$ is the weight of user k , $f(\cdot)$ is assumed to be twice differentiable, concave, and increasing L-Lipschitz function for all $\bar{r} \geq 0$. Solving (10) is non-trivial since the average rate region \mathcal{R} does not have a tractable form. To overcome this challenge, we need to find closed-form expressions of the data rate and the average transmit power.

⁴The Pareto optimal is the set of user rates at which it is impossible to improve any of the rates without simultaneously decreasing at least one of the others.

C. Closed-Form Expression via Deterministic Equivalent

We invoke recent results from RMT in order to get the deterministic equivalent. As $K, N \rightarrow \infty$, by applying the techniques in [6, Theorem 2], for small α the deterministic equivalent of the asymptotic SINRs of UEs (6-7) is

$$\gamma_m^{(b_0)}(\Lambda|\Theta) \xrightarrow{a.s.} \frac{l_m p_m^{(b_0)} (1 - \tau_m^2)}{1 + \sum_{s=1}^S \beta^{(b_s)} \zeta_m^{(b_s)}},$$

$$\gamma_s^{(b_0)}(\Lambda|\Theta) \xrightarrow{a.s.} \frac{l_s p_s^{(b_0)}}{1 + \sum_{s'=1, s' \neq s}^S \beta^{(b_{s'})} \zeta_s^{(b_{s'})}},$$

where $\xrightarrow{a.s.}$ denotes the almost sure convergence, please see the proof in Appendix A. The precoder \mathbf{T} is designed to satisfy a total transmit power constraint and takes into account the scheduling \mathbf{l} and \mathbf{U} , and thus, we obtain $\frac{1}{N} \sum_{k=1}^K \frac{p_k^{(b_0)}}{\Omega_k} - P^{(b_0)} \leq 0$. Here, $\Omega_k = \frac{1}{N} \text{Tr}(\tilde{\Theta}_k \mathbf{G})$ forms the unique positive solution of which is the Stieltjes transform of nonnegative finite measure [6, Theorem 1], where $\mathbf{G} = (\frac{1}{N} \sum_{k=1}^K \frac{\tilde{\Theta}_k}{\alpha + \Omega_k} + \mathbf{I}_{N_i})^{-1}$ and $\tilde{\Theta}_k = \mathbf{U}\mathbf{U}^\dagger \Theta_k^{(b_0)} \mathbf{U}\mathbf{U}^\dagger$.

Although the closed-form expression of time average of data rate and transmit power is obtained, our problem considers a time-average optimization with a large number of control variables and dynamic traffic load over the convex region for a given composite control variable Λ and Θ . Moreover, the goal is to maximize the aggregate network utility subject to queue stability in which the Lyapunov optimization framework can be utilized effectively, by means of drift-plus-penalty technique [10] to solve the joint scheduling and interference mitigation problem.

IV. LYAPUNOV OPTIMIZATION FRAMEWORK

The network operation is modeled as a queueing network that operates in discrete time $t \in \{0, 1, 2, \dots\}$. Let $a_k(t)$ denote the bursty data arrival destined for each user k , i.i.d over time slot t . Let $\mathbf{Q}(t)$ denote the vector of transmission queue backlogs at MBS at slot t . The evolution of $\mathbf{Q}(t)$ is

$$Q_k(t+1) = \max[Q_k(t) - r_k(t), 0] + a_k(t), \forall k \in \mathcal{K}. \quad (11)$$

Here, we define the bound of the traffic arrival of user k such that $0 \leq a_k(t) \leq a_k^{\max}$, for some constant $a_k^{\max} < \infty$. Here, we define the upper bound of traffic data $r_k^{\max}(t) < \infty$ for user k at time slot t . The set constraint (10b) is replaced by an inequivalent set constraint by introducing auxiliary variables $\varphi(t) \in \mathcal{R}$, $\varphi(t) = (\varphi_1(t), \dots, \varphi_K(t))$ that satisfies $\bar{\varphi}_k \leq \bar{r}_k$, where $\bar{\varphi}_k \triangleq \lim_{t \rightarrow \infty} \frac{1}{t} \sum_{\tau=0}^{t-1} \mathbb{E}[\varphi_k(\tau)]$. The wireless backhaul queue can be rewritten as

$$D_s(t+1) = \max[D_s(t) + \varphi_s(t) - r_{c_s}(t), 0]. \quad (12)$$

For a given Λ and Θ , the optimization problem (10) with the network stability can be posed as

$$\min_{\bar{\varphi}} \quad -f_0(\bar{\varphi}) \quad (13a)$$

$$\text{subject to} \quad \bar{\varphi}_k - \bar{r}_k \leq 0, \forall k \in \mathcal{K}, \quad (13b)$$

$$\bar{\mathbf{D}} < \infty, \bar{\mathbf{Q}} < \infty. \quad (13c)$$

In order to ensure the inequality constraint (13b), we introduce a virtual queue vector $\mathbf{Y}(t)$ where

$$Y_k(t+1) = \max[Y_k(t) + \varphi_k(t) - r_k(t), 0]. \quad (14)$$

We define the queue backlog vector as $\Sigma(t) = [\mathbf{Q}(t), \mathbf{Y}(t), \mathbf{D}(t)]$ which involves all constraints of (13). The Lyapunov function can be written as $L(\Sigma(t)) \triangleq$

$\frac{1}{2} [\sum_{k=1}^K Q_k(t)^2 + \sum_{k=1}^K Y_k(t)^2 + \sum_{s=1}^S D_s(t)^2]$. For each time slot t , $\Delta(\Sigma(t))$ denotes the Lyapunov drift given by $\Delta(\Sigma(t)) \triangleq \mathbb{E}[L(\Sigma(t+1)) - L(\Sigma(t)) | \Sigma(t)]$.

Noting that $\max[a, 0]^2 \leq a^2$ and $(a \pm b)^2 \leq a^2 \pm 2ab + b^2$ for any real positive number a, b , and thus, by neglecting the index t we have, $(\max[Q_k - r_k, 0] + a_k)^2 - Q_k^2 \leq 2Q_k(a_k - r_k) + (a_k - r_k)^2$, $\max[Y_k + \varphi_k - r_k, 0]^2 - Y_k^2 \leq 2Y_k(\varphi_k - r_k) + (\varphi_k - r_k)^2$, $\max[D_s + \varphi_s - r_{c_s}, 0]^2 - D_s^2 \leq 2D_s(\varphi_s - r_{c_s}) + (\varphi_s - r_{c_s})^2$. Assume that $\varphi_k \in \mathcal{R}$ and a feasible \mathbf{l} for all t and all possible $\Sigma(t)$, we have

$$\begin{aligned} \Delta(\Sigma(t)) &\leq \Psi + \sum_{k=1}^K Q_k(t) \mathbb{E}[a_k(t) - r_k(t) | \Sigma(t)] \\ &\quad + \sum_{k=1}^K Y_k(t) \mathbb{E}[\varphi_k(t) - r_k(t) | \Sigma(t)] \\ &\quad + \sum_{s=1}^S D_s(t) \mathbb{E}[\varphi_s(t) - r_{c_s}(t) | \Sigma(t)]. \end{aligned} \quad (15)$$

Here $\Delta(\Sigma(t)) \leq \Pi$, where Π represents the R.H.S of (15), and Ψ is a finite constant that satisfies $\Psi \geq \frac{1}{2} \sum_{k=1}^K \mathbb{E}[(a_k(t) - r_k(t))^2 | \Sigma(t)] + \frac{1}{2} \sum_{k=1}^K \mathbb{E}[(\varphi_k(t) - r_k(t))^2 | \Sigma(t)] + \frac{1}{2} \sum_{s=1}^S \mathbb{E}[(\varphi_s(t) - r_{c_s}(t))^2 | \Sigma(t)]$, for all t and all possible $\Sigma(t)$. We apply the Lyapunov drift-plus-penalty technique, where the solution of (13) is obtained by minimizing the Lyapunov drift and the objective function, i.e., $\min \Pi - \nu \mathbb{E}[f_0(\varphi(t))]$, where the parameter ν is chosen as a non-negative constant to control optimality and queue backlogs. Since Ψ is finite, the problem becomes minimizing (16), which is decoupled over scheduling and operation mode variables (1*), auxiliary variables (2*), and precoder and power allocation variables (3*), respectively. Hence, the respective variables can be found independently by minimizing the individual term at each time. Fig. 2 summarizes the relationship among subproblems.

A. Step 1: Joint In-Band Scheduling and FD or HD Operation Mode Control

The joint in-band scheduling and SC operation mode control problem is a mixed-integer program with a non-convex objective function and non-convex interference constraints. To solve this problem, we first relax the integer constraints to linear constraints as continuous values. Secondly, to deal with non-convex interference constraint, we apply the SCA method [11, Lemma 3.5], where at each iteration i the non-convex constraints are approximated by upper convex approximations. Hence, we solve iteratively the problem by updating the variables until convergence to obtain a Karush-Kuhn-Tucker (KKT) point. The interference constraint is replaced by $\sum_{i=1}^K \sum_{s=1}^S (\frac{\lambda_{ks}^{(i)} l_k^2(t)}{2} + \frac{(\beta^{(b_s)})^2(t)}{2\lambda_{ks}^{(i)}}) \zeta_k^{(b_s)}(t) - \epsilon_o \leq 0$, for every fixed positive value $\lambda_{ks}^{(i)}$. Finally, instead of minimizing the non-convex objective function (2*), we minimize its upper bound by replacing the denominators, i.e., $1 + \sum_{s=1}^S \beta^{(b_s)} \zeta_m^{(b_s)}$ with the largest bound, i.e., $1 + \epsilon_o$. This upper bound is obtained due to interference constraint $\sum_{i=1}^K \sum_{s=1}^S l_i \beta^{(b_s)} \zeta_i^{(b_s)} \leq \epsilon_o$ and we assume the feasibility of problem exists such that the total FD interference at each receiver is less than the total FD interference threshold ϵ_o . Hence, we obtain the upper bound as below and the optimal value of Λ^o is given by

$$\left[\left[-\sum_k (Q_k(t) + Y_k(t)) r_k(\boldsymbol{\Lambda}(t)) \right]_{3\star} \left[-\sum_s D_s(t) r_{c_s}(\beta^{(b_s)}(t)) \right]_{1\star} + \left[\sum_k Y_k(t) \varphi_k(t) + \sum_s D_s(t) \varphi_s(t) - \nu f_0(\boldsymbol{\varphi}(t)) \right]_{2\star} \right]_{16}.$$

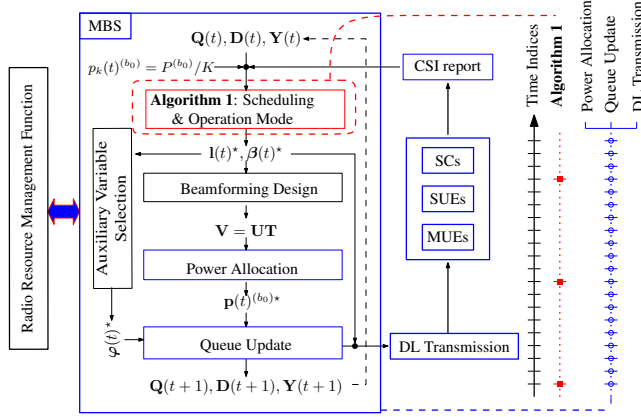


Fig. 2: Joint Scheduling and Interference Mitigation Algorithm.

$$\begin{aligned} \min_{\mathbf{l}, \beta} \quad & -\sum_{s=1}^S D_s(t) \log \left(1 + \frac{\beta^{(b_s)}(t) p_{c_s}^{(b_s)} |h_{c_s}^{(b_s)}|^2}{1 + \epsilon_0} \right) \\ & -\sum_{k=1}^K A_k(t) \log \left(1 + \frac{l_k(t) p_k^{(b_0)} (1 - \tau_k^2)}{1 + \epsilon_0} \right) \quad (17a) \\ \text{subject to} \quad & l_k(t), \beta^{(b_s)}(t) \in [0, 1], \forall k \in \mathcal{K}, \forall s \in \mathcal{S}, \quad (17b) \\ & \sum_{k=1}^K l_k(t) + \sum_{s=1}^S \beta^{(b_s)}(t) \leq N, \quad (17c) \\ & \sum_{i=1}^K \sum_{s=1}^S \left(\frac{\lambda_{k_s}^{(i)} l_k^2(t)}{2} + \frac{(\beta^{(b_s)}(t))^2}{2\lambda_{k_s}^{(i)}} \right) \zeta_k^{(b_s)}(t) \leq \epsilon_0, \quad (17d) \\ & r_k(l_k(t), \beta^{(b_s)}(t)) \in \mathcal{R}, \quad (17e) \end{aligned}$$

where $A_k(t) = Q_k(t) + Y_k(t)$. At each time slot t , the joint in-band scheduling and SC operation mode control problem is outlined as Algorithm 1. We numerically observe that the SCA-based Algorithm 1 converges quickly after few iterations and yields a solution of many scheduling and operation variables close or equal to binary. Hence, we apply a binary search algorithm in order to obtain a low-complexity search algorithm to convert the continuous relaxation solution to the integer solution [12]. To ensure that all users will be served, each user is set to have the same transmit power to find the best scheduled users. Moreover, the scheduling will be performed in a long-term period, while the power allocation problem is executed in a short-term period.

Algorithm 1 Joint in-band scheduling and SC operation mode control problem

Initialization $i = 0$, $\lambda_{k_s}^{(i)}$ = randomly positive.
repeat
 Solve (17) with $\lambda_{k_s}^{(i)}$ to get optimal value $\boldsymbol{\Lambda}^{o\star}$.
 Update $\boldsymbol{\Lambda}^{o(i)} := \boldsymbol{\Lambda}^{o\star}$ and $\lambda_{k_s}^{(i+1)} := \frac{\beta^{(b_s)}(t)}{l_k^{(i)}}$; $i := i + 1$.
until Convergence

B. Step 2: Selection of Auxiliary Variable

The optimal auxiliary variables are computed by

$$\min_{\boldsymbol{\varphi}(t)} \quad \sum_{k=1}^K Y_k(t) \varphi_k(t) + \sum_{s=1}^S D_s(t) \varphi_s(t) - \nu f_0(\boldsymbol{\varphi}(t)), \quad (18a)$$

$$\text{subject to} \quad \varphi_k(t) \leq r_k^{\max}(t). \quad (18b)$$

Since the above optimization problem is convex, let $\varphi_k^*(t)$ be the optimal solution obtained by the first order derivative of the objective function of (18). With a logarithmic utility function, we have:

$$\varphi_k^*(t) = \begin{cases} \frac{\nu \omega_k(t)}{Y_k(t)} & \text{if } k \leq M, \\ \frac{\nu \omega_k(t)}{Y_k(t) + D_{k-M}(t)} & \text{otherwise.} \end{cases}$$

The optimal auxiliary variable is $\min\{\varphi_k^*(t), r_k^{\max}(t)\}$.

C. Step 3: Interference Mitigation and Power Allocation

For given scheduled users in *Step 1*, the precoder \mathbf{U} is found by solving (2). Finally, problem (13) is decomposed to find the transmit power $p_k^{(b_0)}(t)$ as follows:

$$\min_{\mathbf{p}(t)} \quad -\sum_{k=1}^K A_k(t) r_k(\mathbf{p}(t)), \quad (19a)$$

$$\text{subject to} \quad \frac{1}{N} \sum_{k=1}^K \frac{p_k^{(b_0)}(t)}{\Omega_k(t)} - P^{(b_0)} \leq 0, \quad (19b)$$

$$p_k^{(b_0)}(t) \geq 0, \forall k \in \mathcal{K}. \quad (19c)$$

The objective function (19) is rewritten as $n(\mathbf{p}(t)) = -\sum_{k=1}^K A_k(t) \log \left(1 + \frac{p_k^{(b_0)}(t) n_k(t)}{l_k(t) (1 - \tau_k^2)} \right)$, where $n_k(t) = \frac{1}{1 + \sum_{s=1}^S \beta^{(b_s)}(t) \zeta_k^{(b_s)}(t)}$. The objective function is strictly convex for $p_k^{(b_0)}(t) \geq 0, \forall k \in \mathcal{K}$, and the constraints are compact. Hence, the optimal solution of $\mathbf{p}^*(t)$ exists, the Lagrangian function is written as $\mathcal{L}(\mathbf{p}(t), \mu_0) = n(\mathbf{p}(t)) + \mu_0 \mathbf{g}(\mathbf{p}(t))$, where $\mu_0 \geq 0$ is the KKT multiplier. The KKT conditions are

$$\nabla n(\mathbf{p}(t))^T + \mu_0 \frac{1}{N} \sum_{k=1}^K \frac{1}{\Omega_k(t)} = 0. \quad (20)$$

$$\mu_0 \left(\frac{1}{N} \sum_{k=1}^K \frac{p_k^{(b_0)}(t)}{\Omega_k(t)} - P^{(b_0)} \right) = 0. \quad (21)$$

$$\frac{1}{N} \sum_{k=1}^K \frac{p_k^{(b_0)}(t)}{\Omega_k(t)} - P^{(b_0)} \leq 0. \quad (22)$$

$$-\mathbf{p}(t) \leq 0, \mu_0 \geq 0. \quad (23)$$

Here, $\nabla n(\mathbf{p}(t))^T = (n'(p_1^{(b_0)}(t)), \dots, n'(p_K^{(b_0)}(t)))$ where $n'(p_k^{(b_0)}(t)) = \frac{-A_k(t) n_k(t)}{1 + p_k^{(b_0)}(t) n_k(t)}$. Since $\mu_0 \neq 0$, from (20), we have

$$p_k^{(b_0)}(t) = \max \left[\frac{A_k N \Omega_k(t)}{\mu_0} - \frac{1}{n_k(t)}, 0 \right], \quad (24)$$

then, from (21) and (24) we derive μ_0 . Finally, the optimal value of $p_k(t)^{(b_0)\star}$ is obtained with (24).

D. Queue Update

Update the virtual queues $Y_k(t)$ and $D_s(t)$ according to (14) and (12), and the actual queue $Q_k(t)$ in (11).

TABLE I: Parameter Settings

Path Loss Model [13]	Values in dB	Bandwidth (BW) in MHz
LOS @ 2.4 GHz	$17 + 37.6 \log(d)$	20
LOS @ 10 GHz	$55.25 + 18.5 \log(d)$	100
LOS @ 28 GHz	$61.4 + 20 \log(d)$	1000
Parameter		Values
Maximum transmit power of MBS $P^{(b_0)}$	43 dBm	
Maximum transmit power of SC	23 dBm	
FD interference threshold ϵ_o	5×10^{-3}	
Channel estimate error τ	0.1	
SC Antenna Gain	5 dBi	
Lyapunov parameter ν	$2 \times 10^3/1$ MHz BW	
RZF parameter α	10^{-2}	

V. NUMERICAL RESULTS

We consider a HetNet scenario, where a MBS is located at the center of the cell. The path loss is modeled as a distance-based path loss with line-of-sight (LOS) model for urban environments at 28 GHz, 10 GHz, and 2.4 GHz [13]. We denote our proposed algorithms for HetNet (resp. Homogeneous network) as HetNet-Hybrid (resp. HomNet). Here, HomNet refers to when the MBS serves both MUEs and SUEs without SCs. The data arrivals follow the Poisson distribution with the mean rate of 1 Gbps, 100 Mbps, and 20 Mbps for 28 GHz, 10 GHz, and 2.4 GHz, respectively. We consider the proportional fairness utility function, i.e., $f(\tilde{r}_k) = \log \tilde{r}_k$ [14]. The parameter settings are summarized in Table I.

Fig. 3 and 4 report the achievable average UE throughput, cell-edge UE throughput, and average network queue length as a function of network density at different frequency bands. The number of SCs S increases from 16 to 900, reflecting the inter-site distance (ISD) between SCs decreasing from 250 m to 33 m. On the other hand, the number of UEs K increases from 32 UEs to 1800 UEs per km^2 . Moreover, the number of antennas N at the MBS is twice the number of UEs K .

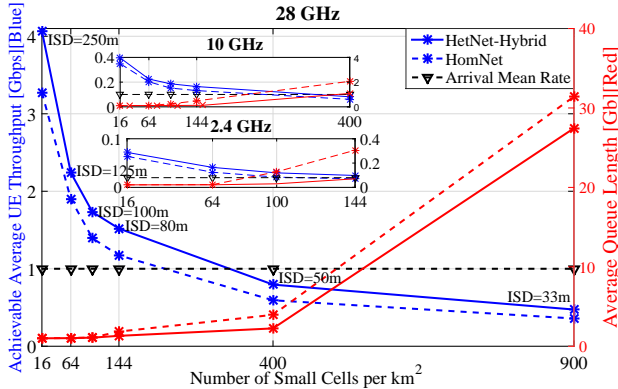


Fig. 3: Achievable Average UE throughput and Network Queue length versus number of Small Cells at 28 GHz, 10 GHz, and 2.4 GHz.

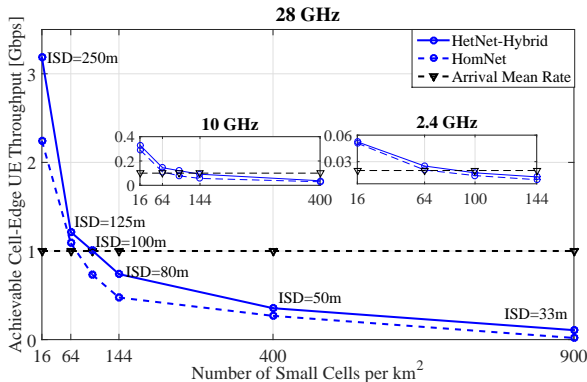


Fig. 4: Achievable 5th% UE throughput versus number of Small Cells at 28 GHz, 10 GHz, and 2.4 GHz.

With the increase in the number of SCs S and MUEs M , the per UE/SC transmit power is reduced by a factor of K and the cross-tier interference becomes dominant. Hence, the achievable average UE throughput gradually decreases, while the network queue traffic becomes more congested. Moreover, the UE throughput at 28 GHz achieves $56\times$ and $62\times$ gain as compared to 2.4 GHz due to $50\times$ larger bandwidth and smart beamforming, when the ISD is 250 m and 80 m, respectively. In ultra-dense deployment, the UE throughput at 2.4 GHz is below 10 Mbps, whereas 473 Mbps per UE is achieved by using 28 GHz for 33 m of ISD.

By taking advantage of mmWave frequency bands, we observe that at 28 GHz when the number of UEs per km^2 is increased to 200 UEs, the average UE throughput reaches **1.73 Gbps** and **1.39 Gbps** in case of **HetNet-Hybrid** and **HomNet**, respectively. Whereas the cell-edge UE throughput reaches **1 Gbps** and **0.73 Gbps** in case of **HetNet-Hybrid** and **HomNet**, respectively. When the ISD is less than 50 m, the network queue size dramatically increases, and the network becomes congested. To handle this problem, the arrival traffic needs to be adjusted by reducing the admitting data or the UE throughput should increase by increasing the maximum BS transmit power and number of antennas.

The performance of NUM based on Lyapunov framework is analyzed in [10]. There exists an $[\mathcal{O}(1/\nu), \mathcal{O}(\nu)]$ utility-queue backlog tradeoff, which leads to an utility-delay tradeoff. We show the impact of the Lyapunov parameter ν on the achievable average network utility and queue backlog as seen in Fig. 5, when $K = 16$, $N = 64$, and $P^{(b_0)} = 38$ dBm. By varying the value of ν , the network utility is increasing with $\mathcal{O}(1/\nu)$, while the network backlog linearly increases with $\mathcal{O}(\nu)$.

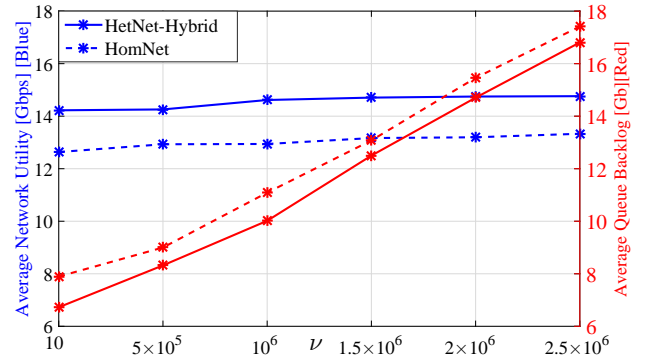


Fig. 5: Impact of ν on the Utility and Network Backlogs at 28 GHz when $K = 16$, $N = 64$.

VI. CONCLUSION

In this paper, we have studied the problem of joint in-band backhaul scheduling and interference mitigation in 5G HetNets which takes into account the combination of in-band FD-SC and massive MIMO technologies. The main addressed problem is to simultaneously schedule macro cell users and to provide the wireless backhaul to small cells. The goal is to maximize a network utility function of the total time-average data rates subject to the wireless backhaul constraint and network stability in the presence of imperfect CSI. At mmWave 28 GHz with 1 GHz of BW, we observe that **1.7 Gbps** of the achievable average UE throughput and **1 Gbps** of the cell-edge UE throughput can be reached for 200 UE per km^2 in HetNet. When the network gets dense, harnessing mmWave yields $62\times$ gain of UE throughput as compared to conventional cellular frequency.

APPENDIX
PROOF OF CLOSED-FORM EXPRESSION

By applying the technique in [6, Theorem 2, 3], the deterministic equivalent of the asymptotic SINR of the MUE m is

$$\gamma_m^{(b_0)} \xrightarrow{a.s.} \frac{l_m p_m^{(b_0)} (1 - \tau_m^2) (\Omega_m)^2}{\Phi},$$

where $\Phi = \Upsilon_m \left[\alpha^2 - \tau_m^2 (\alpha^2 - (\alpha + \Omega_m)^2) \right] + (\alpha + \Omega_m)^2 (1 + \sum_{s=1}^S \beta^{(b_s)} \zeta_m^{(b_s)})$. $\Omega_m = \frac{1}{N} \text{Tr}(\tilde{\Theta}_m \mathbf{G})$ forms the unique positive solution of which is the Stieltjes transform of nonnegative finite measure, where $\mathbf{G} = \left(\frac{1}{N} \sum_{k=1}^K \frac{\tilde{\Theta}_k}{\alpha + \Omega_k} + \mathbf{I}_{N_i} \right)^{-1}$.

Here, $\Upsilon_m = \frac{1}{N} \sum_{k=1, k \neq m}^K \frac{\alpha^2 l_k p_k^{(b_0)} e_{km}}{(\alpha + \Omega_k)^2}$, and, where $\tilde{\Theta}_k = \mathbf{U} \mathbf{U}^\dagger \Theta_k^{(b_0)} \mathbf{U} \mathbf{U}^\dagger$. $\mathbf{e} = [e_k]$, $k \in \mathcal{K}$, and $\mathbf{e}_m = [e_{mk}]$, $k \in \mathcal{K}$ are given by $\mathbf{e} = (\mathbf{I} - \mathbf{J})^{-1} \mathbf{u}$, $\mathbf{e}_k = (\mathbf{I} - \mathbf{J})^{-1} \mathbf{u}_k$, where $\mathbf{J} = [J_{ij}]$, $i, j \in \mathcal{K}$. $\mathbf{u} = [u_k]$, $k \in \mathcal{K}$, $\mathbf{u}_m = [u_{mk}]$, $k \in \mathcal{K}$ are given by $J_{ij} = \frac{\frac{1}{N} \text{tr} \tilde{\Theta}_i \mathbf{G} \tilde{\Theta}_j \mathbf{G}}{N(\alpha + \Omega_j)^2}$, $u_{mk} = \frac{1}{\alpha^2 N} \text{tr} \tilde{\Theta}_k \mathbf{G} \tilde{\Theta}_m \mathbf{G}$, $u_k = \frac{1}{\alpha^2 N} \text{tr} \tilde{\Theta}_k \mathbf{G}^2$. Similarly, the SINR of the SC b_s are

$$\gamma_s^{(b_0)} \xrightarrow{a.s.} \frac{l_s p_s^{(b_0)} (\Omega_s)^2}{\alpha^2 \Upsilon_s + (\alpha + \Omega_s)^2 (1 + \sum_{s'=1, s' \neq s}^S \beta^{(b_{s'})} \zeta_s^{(b_{s'})})}.$$

REFERENCES

- [1] "2020: Beyond 4g radio evolution for the gigabit experience," White Paper, Nokia Siemens Networks, 2011.
- [2] T. L. Marzetta, "Noncooperative cellular wireless with unlimited numbers of base station antennas," *IEEE Transactions on Wireless Communications*, vol. 9, no. 11, pp. 3590–3600, 2010.
- [3] B. Li, D. Zhu, and P. Liang, "Small cell in-band wireless backhaul in massive multiple-input multiple-output systems," in *IEEE International Conference on Communications*, 2015.
- [4] L. Sanguinetti, A. Moustakas, and M. Debbah, "Interference management in 5G reverse TDD HetNets: A large system analysis," *IEEE Journal on Selected Areas in Communications*, vol. 33, pp. 1187–1200, 2015.
- [5] F. Rusek, D. Persson, B. Lau, E. Larsson, T. Marzetta, O. Edfors, and F. Tufvesson, "Scaling up MIMO: Opportunities and challenges with very large arrays," *IEEE Signal Processing Magazine*, vol. 30, no. 1, pp. 40–60, 2013.
- [6] S. Wagner, R. Couillet, M. Debbah, and D. Slock, "Large system analysis of linear precoding in correlated MISO broadcast channels under limited feedback," *IEEE Transactions on Information Theory*, vol. 58, no. 7, pp. 4509–4537, 2012.
- [7] A. Liu and V. Lau, "Hierarchical Interference Mitigation for Massive MIMO Cellular Networks," *IEEE Transactions on Signal Processing*, vol. 62, no. 18, pp. 4786–4797, Sept 2014.
- [8] H. Boche, S. Naik, and M. Schubert, "Pareto boundary of utility sets for multiuser wireless systems," *IEEE/ACM Transactions on Networking*, vol. 19, no. 2, pp. 589–601, 2011.
- [9] Z. Chen, S. Vorobyov, C. Wang, J. Thompson *et al.*, "Pareto region characterization for rate control in MIMO interference systems and Nash bargaining," *IEEE Transactions on Automatic Control*, vol. 57, no. 12, pp. 3203–3208, 2012.
- [10] M. J. Neely, "Stochastic network optimization with application to communication and queueing systems," *Synthesis Lectures on Communication Networks*, vol. 3, no. 1, pp. 1–211, 2010.
- [11] A. Beck, A. Ben-Tal, and L. Tretuashvili, "A sequential parametric convex approximation method with applications to nonconvex truss topology design problems," *Journal of Global Optimization*, vol. 47, no. 1, pp. 29–51, 2010.
- [12] H. Li, L. Song, and M. Debbah, "Energy efficiency of large-scale multiple antenna systems with transmit antenna selection," *IEEE Transactions on Communications*, vol. 62, no. 2, pp. 638–647, 2014.
- [13] M. R. Akdeniz, Y. Liu, M. K. Samimi, S. Sun, S. Rangan, T. S. Rappaport, and E. Erkip, "Millimeter wave channel modeling and cellular capacity evaluation," *IEEE Journal on Selected Areas in Communications*, vol. 32, no. 6, pp. 1164–1179, 2014.

- [14] J. Mo and J. Walrand, "Fair end-to-end window-based congestion control," *IEEE/ACM Transactions on Networking (ToN)*, vol. 8, no. 5, pp. 556–567, 2000.